

# Muon $g - 2$ : a mini review

Zhiqing Zhang

*LAL, Univ Paris-Sud, CNRS/IN2P3, Orsay, France*

The current status of the experimental measurements and theoretical predictions of the anomalous magnetic moment of the muon  $a_\mu$  is briefly reviewed. The emphasis is put on the evaluation of the hadronic contribution to  $a_\mu$  as it has the largest uncertainty among all Standard Model contributions. The precision of the hadronic contribution is driven by the input  $e^+e^-$  data predominantly from the  $\pi^+\pi^-$  channel. Including the latest experimental data on  $e^+e^-$  annihilation into hadrons from CMD2 and SND for the  $\pi^+\pi^-$  channel and BABAR for multihadron final states, the updated Standard Model prediction disagrees with the measurement dominated by BNL by 3.3 standard deviations, with the theoretical precision exceeding the experimental one.

## 1 Introduction

For a charged elementary particle with  $1/2$  intrinsic spin such as muon, its magnetic dipole moment  $\vec{\mu}$  is aligned with its spin  $\vec{s}$  as:

$$\vec{\mu} = g \left( \frac{q}{2m} \right) \vec{s}, \quad (1)$$

where  $q = \pm e$  is the charge of the particle in unit of the electron charge and  $g$  is the gyromagnetic ratio. In the classic Dirac theory,  $g = 2$ . In the Standard Model (SM), quantum loop effects induce a small correction, which is quantified by  $a_\mu = (g_\mu - 2)/2$ , the so-called anomalous magnetic moment or the magnetic anomaly.

There has been a long history in measuring and calculating  $a_\mu$ . In particular the steadily improving precision of both the measurements and the predictions of  $a_\mu$  and the disagreement observed between the two have led the study of  $a_\mu$  one of the most active research fields in particle physics in recent years.

The paper is organized as follows. In section 2, the measurement history and the current world average value of  $a_\mu$  are presented. In section 3, different components of the SM contributions to  $a_\mu$  are reviewed. Section 4 is reserved for discussions followed by conclusion and prospects in section 5.

## 2 The Measurement of $a_\mu$

A compilation of the major experimental efforts in measuring  $a_\mu$  over the last five decades is given in Table 1 (a modified version of Table 1 from a recent review article<sup>1</sup>). Starting from the experiment at the Columbia-Nevis cyclotron, where the spin rotation of a muon in a magnetic field was observed for the first time, the experimental precision of  $a_\mu$  has seen constant improvement first through three experiments at CERN in the sixties and seventies and more recently with E821 at the Brookhaven National Laboratory (BNL). The current world average value reaches a relative precision of 0.54 ppm (parts per million).

Table 1: Measurements of the muon magnetic anomaly  $a_\mu$ , where the value in parentheses stands for either the total experimental error or the statistical and systematic ones.

Experiment	Beam	Measurement	$\delta a_\mu/a_\mu$
Columbia-Nevis(1957) <sup>2</sup>	$\mu^+$	$g = 2.00 \pm 0.10$	
Columbia-Nevis(1959) <sup>3</sup>	$\mu^+$	$0.001\,13^{+(16)}_{-(12)}$	12.4%
CERN 1(1961) <sup>4</sup>	$\mu^+$	0.001 145(22)	1.9%
CERN 1(1962) <sup>5</sup>	$\mu^+$	0.001 162(5)	0.43%
CERN 2(1968) <sup>6</sup>	$\mu^\pm$	0.001 166 16(31)	265 ppm
CERN 3(1975) <sup>7</sup>	$\mu^\pm$	0.001 165 895(27)	23 ppm
CERN 3(1979) <sup>8</sup>	$\mu^\pm$	0.001 165 911(11)	7.3 ppm
BNL E821(2000) <sup>9</sup>	$\mu^+$	0.001 165 919 1(59)	5 ppm
BNL E821(2001) <sup>10</sup>	$\mu^+$	0.001 165 920 2(16)	1.3 ppm
BNL E821(2002) <sup>11</sup>	$\mu^+$	0.001 165 920 3(8)	0.7 ppm
BNL E821(2004) <sup>12</sup>	$\mu^-$	0.001 165 921 4(8)(3)	0.7 ppm
World Average(2004) <sup>12,13</sup>	$\mu^\pm$	0.001 165 920 80(63)	0.54 ppm

The muon magnetic anomaly  $a_\mu$  in all modern experiments is determined by the following method. For an ensemble of polarized muons which are moving in a storage ring in a highly uniform magnetic field  $\vec{B}$  (perpendicular to muon spin and orbit plane) and a vertically focusing quadrupole field  $\vec{E}$ , the frequency difference  $\omega_a$  between the spin precession  $\omega_s$  and the cyclotron motion  $\omega_c$  is described by

$$\vec{\omega}_a \equiv \vec{\omega}_s - \vec{\omega}_c = \frac{e}{m_\mu c} \left[ a_\mu \vec{B} - \left( a_\mu - \frac{1}{\gamma^2 - 1} \right) (\vec{\beta} \times \vec{E}) \right], \quad \text{when } \vec{B} \cdot \vec{\beta} = \vec{E} \cdot \vec{\beta} = 0 \quad (2)$$

where  $\vec{\beta}$  represents the muon direction. The second term in parentheses vanishes at  $\gamma = 29.3$  (the magic momentum) and the electrostatic focusing does not affect the spin. The key to the experiment is to determine frequency  $\omega_a$  to high precision and to measure the average magnetic field to equal or better precision.

In comparison with the electron magnetic anomaly,  $a_e$  is more precisely measured<sup>14</sup> (0.7 ppb), but  $a_\mu$  is more sensitive to new physics effects by about  $m_\mu^2/m_e^2 \simeq 40\,000$  because of its large mass value.

## 3 Prediction of the Standard Model Contributions

In the SM, the muon magnetic anomaly  $a_\mu$  receives contributions from all electromagnetic (QED), weak and strong (hadronic) sectors and can be conveniently written as:

$$a_\mu^{\text{SM}} = a_\mu^{\text{QED}} + a_\mu^{\text{weak}} + a_\mu^{\text{had}}. \quad (3)$$

Their representative diagrams are shown in Fig. 1, which also includes two example contributions from new particles in supersymmetry models. Thus comparison of the precision measurement and theory tests the validity of the SM at its quantum loop level and probes effects of new physics.

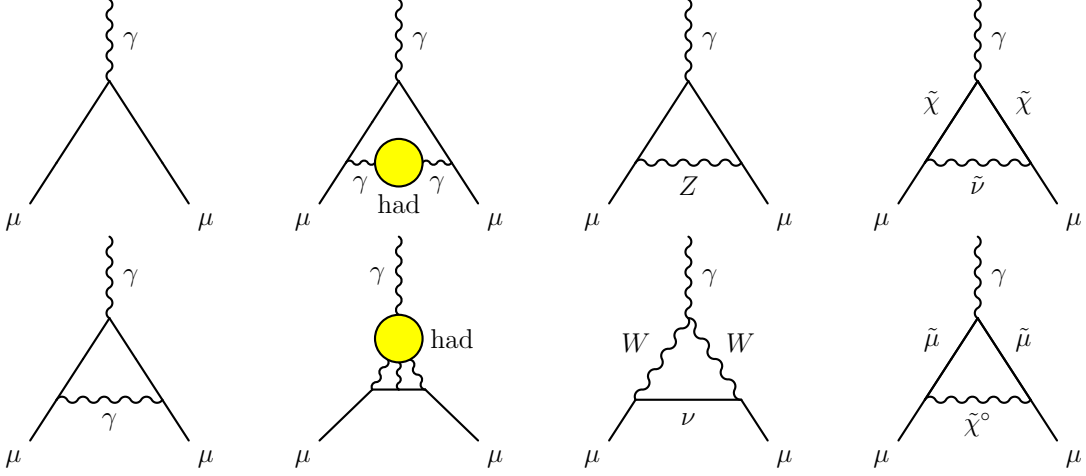


Figure 1: Representative diagrams contributing to  $a_\mu$ . First column: lowest-order diagram (upper) and first order QED correction (lower); second column: lowest-order hadronic contribution (upper) and hadronic light-by-light scattering (lower); third column: weak interaction diagrams; last column: possible contributions from lowest-order Supersymmetry.

### 3.1 QED and Weak Contributions

The QED correction, which includes all photonic and leptonic ( $e$ ,  $\mu$  and  $\tau$ ) loops, is by far the dominant contribution in the SM:

$$a_\mu^{\text{QED}} = \frac{\alpha}{2\pi} + 0.765\,857\,410(27) \left(\frac{\alpha}{\pi}\right)^2 + 24.050\,509\,64(43) \left(\frac{\alpha}{\pi}\right)^3 + 130.9916(80) \left(\frac{\alpha}{\pi}\right)^4 + 663(20) \left(\frac{\alpha}{\pi}\right)^5 + \dots, \quad (4)$$

where the lowest-order Schwinger term ( $\alpha/2\pi$ ) was known since 1948<sup>16</sup>, the coefficients are analytically known for terms up to  $(\alpha/\pi)^3$ , numerically calculated for the fourth term and recently estimated for the fifth term<sup>15</sup>. Using  $\alpha$  extracted from the latest  $a_e$  measurement<sup>14</sup>, one has

$$a_\mu^{\text{QED}} = 116\,584\,718.09(0.14)_{5\text{th order}}(0.08)_{\delta\alpha} \times 10^{-11}. \quad (5)$$

The weak contributions, involving heavy  $Z$ ,  $W^\pm$  or Higgs particles, are suppressed by at least a factor  $\frac{\alpha}{\pi} \frac{m_\mu^2}{M_W^2} \simeq 4 \times 10^{-9}$ . At one-loop order,

$$a_\mu^{\text{weak}}[1\text{-loop}] = \frac{G_\mu m_\mu^2}{8\sqrt{2}\pi^2} \left[ \frac{5}{3} + \frac{1}{3} (1 - 4\sin^2\theta_W)^2 + \mathcal{O}\left(\frac{m_\mu^2}{M_W^2}\right) + \mathcal{O}\left(\frac{m_\mu^2}{M_H^2}\right) \right] \quad (6)$$

$$= 194.8 \times 10^{-11}, \quad \text{for } \sin^2\theta_W \equiv 1 - \frac{M_W^2}{M_Z^2} \simeq 0.223. \quad (7)$$

Two-loop corrections are relatively large and negative

$$a_\mu^{\text{weak}}[2\text{-loop}] = -40.7(1.0)(1.8) \times 10^{-11}, \quad (8)$$

where the errors stem from quark triangle loops and the assumed Higgs mass range  $M_H = 150_{-40}^{+100}$  GeV. The three-loop leading logarithms are negligible,  $\mathcal{O}(10^{-12})$ , implying in total

$$a_\mu^{\text{weak}} = 154(1)(2) \times 10^{-11}. \quad (9)$$

### 3.2 Hadronic Contributions

The hadronic contributions are associated with quark and gluon loops. They cannot be calculated from first principles because of the low energy scale involved. Fortunately, owing to unitarity and to the analyticity of the vacuum polarization function, the lowest-order hadronic vacuum polarization contribution to  $a_\mu$  can be computed via the dispersion integral<sup>17</sup> using the ratio  $R^{(0)}(s)$  of the bare cross section<sup>a</sup> for  $e^+e^-$  annihilation into hadrons to the pointlike muon pair cross section at center-of-mass energy  $\sqrt{s}$

$$a_\mu^{\text{had,LO}} = \frac{1}{3} \left( \frac{\alpha}{\pi} \right)^2 \int_{m_\pi^2}^{\infty} ds \frac{K(s)}{s} R^{(0)}(s), \quad (10)$$

where  $K(s)$  is the QED kernel<sup>18</sup>  $K(s) = x^2 \left(1 - \frac{x^2}{2}\right) + (1+x)^2 \left(1 + \frac{1}{x^2}\right) \left[\ln(1+x) - x + \frac{x^2}{2}\right] + x^2 \ln x \frac{1+x}{1-x}$ , with  $x = \frac{1-\beta_\mu}{1+\beta_\mu}$  and  $\beta_\mu = \left(1 - \frac{4m_\mu^2}{s}\right)^{1/2}$ . The kernel function  $K(s) \sim \frac{1}{s}$  gives weight to the low energy part of the integral. About 91% of the total contribution to  $a_\mu^{\text{had,LO}}$  is accumulated at  $\sqrt{s}$  below 1.8 GeV and 73% of  $a_\mu^{\text{had,LO}}$  is covered by the  $\pi\pi$  final state, which is dominated by the  $\rho(770)$  resonance.

A detailed compilation of all the experimental data used in the evaluation of the dispersion integral prior to 2004 is provided in Refs.<sup>20,21</sup>. Since then, a few precise measurements have been published. A list of experiments for the dominant  $\pi\pi$  channel is shown in Table 2.

Table 2: A list of measurements of  $e^+e^-$  annihilation into hadrons in the  $\pi^+\pi^-(\gamma)$  channel.

Experiment	$N_{\text{data}}$	Energy range (GeV)	$\delta(\text{stat.})$	$\delta(\text{syst.})$
DM1 (1978) <sup>22</sup>	16	0.483 – 1.096	(6.6 – 40)%	2.2%
TOF (1981) <sup>23</sup>	4	0.400 – 0.460	(14 – 20)%	5%
OLYA (1979, 1985) <sup>24,25</sup>	2 + 77	0.400 – 1.397	(2.3 – 35)%	4%
CMD (1985) <sup>25</sup>	24	0.360 – 0.820	(4.1 – 10.8)%	2%
DM2 (1989) <sup>26</sup>	17	1.350 – 2.215	(17.6 – 100)%	12%
CMD2 (2003) <sup>27</sup>	43	0.611 – 0.962	(1.8 – 14.1)%	0.6%
KLOE (2005) <sup>28</sup>	60	0.600 – 0.970	(0.5 – 2.1)%	(1.2 – 3.8)%
SND (2006) <sup>29</sup>	45	0.390 – 0.970	(0.5 – 2.1)%	(1.2 – 3.8)%
CMD2 <sub>low</sub> (2006) <sup>30</sup>	10	0.370 – 0.520	(4.5 – 7)%	0.7%
CMD2 <sub>rho</sub> (2006) <sup>31</sup>	29	0.600 – 0.970	(0.5 – 4.1)%	0.8%
CMD2 <sub>high</sub> (2006) <sup>32</sup>	36	0.980 – 1.380	(4.5 – 18.4)%	(1.2 – 4.2)%

The  $\pi\pi$  data are compared in Fig. 2. Closer inspections show that the most precise measurements from the annihilation experiments SND and CMD2 at Novosibirsk are in good agreement. They differ however in shape with those measured by KLOE using the radiative return method at DAΦNE<sup>28</sup> (see Sec. 4.1). Before this is clarified, the KLOE data are not used in some of the recent evaluations of  $a_\mu^{\text{had,LO}}$ .

<sup>a</sup>The bare cross section is defined as the measured cross section corrected for initial state radiation, electron vertex contributions and vacuum polarization effects in the photon propagator but with photon radiation in the final state included<sup>19</sup>.

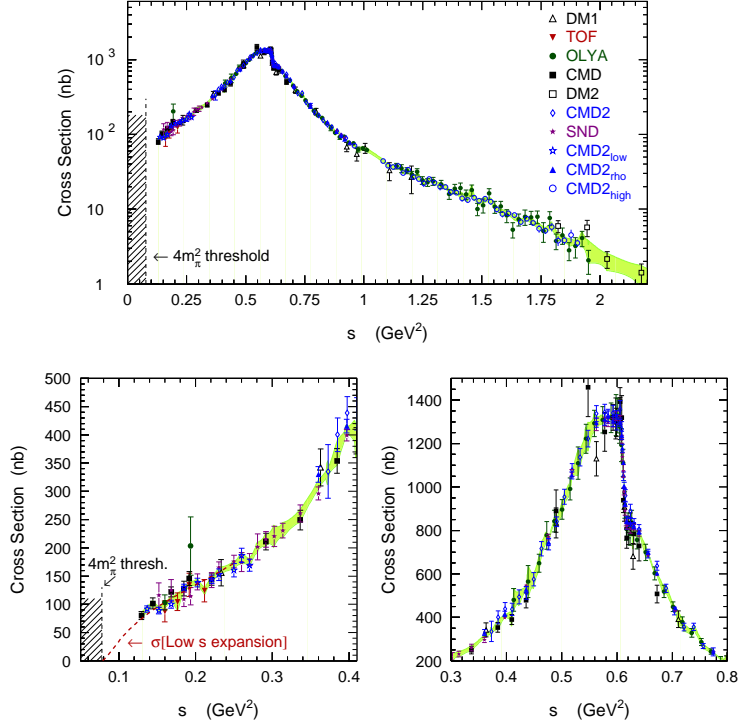


Figure 2: Comparison of  $\pi^+\pi^-$  spectral functions expressed as  $e^+e^-$  cross sections. The band corresponds to combined data used in the numerical integration.

In addition to the dominant  $\pi\pi$  mode, results from the BABAR experiments are being produced on multihadron final states using also radiative return<sup>33</sup>. Benefiting from its big initial center-of-mass energy of 10.6 GeV, hard-radiated photon detected at large angle and high statistics data sample, the BABAR measurements are precise over the whole mass range. One example is shown in Fig. 3 in comparison with earlier measurements.

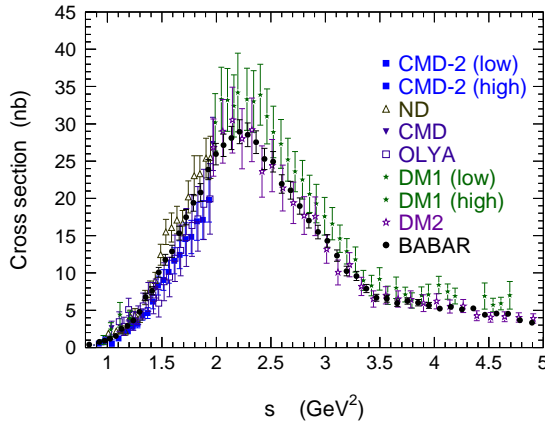


Figure 3: The measured cross section for  $e^+e^- \rightarrow 2\pi^+2\pi^-$  from BABAR compared to previous measurements.

Including these new input  $e^+e^-$  data, a preliminary update<sup>b</sup> of  $a_\mu^{\text{had,LO}}$  is performed<sup>40</sup> and shown in Table 3. There is no new tau data since the previous evaluation, therefore the  $\tau$  based calculation is taken directly from Ref. <sup>21</sup>. The evaluation using  $\tau$  data is made<sup>34</sup> by relating the vector spectral functions from  $\tau \rightarrow \nu_\tau + \text{hadrons}$  decays to isovector  $e^+e^- \rightarrow \text{hadrons}$  cross sections by isospin rotation. All known isospin breaking effects are then taken into account<sup>20,21</sup>.

<sup>b</sup>It is preliminary as some of the new  $e^+e^-$  data used were still in their preliminary form.

Table 3: Summary of the  $a_\mu^{\text{had,LO}}$  contributions from  $e^+e^-$  annihilation and  $\tau$  decays.

Modes	Energy [GeV]	$a_\mu^{\text{had,LO}}(e^+e^-)[10^{-10}]$	$a_\mu^{\text{had,LO}}(\tau)[10^{-10}]$
Low $s$ expansion	$2m_\pi - 0.5$	$55.6 \pm 0.8 \pm 0.1_{\text{rad}}$	$56.0 \pm 1.6 \pm 0.3_{\text{SU}(2)}$
$\pi^+\pi^-$	$0.5 - 1.8$	$449.0 \pm 3.0 \pm 0.9_{\text{rad}}$	$464.0 \pm 3.0 \pm 2.3_{\text{SU}(2)}$
$\pi^+\pi^-2\pi^0$	$2m_\pi - 1.8$	$16.8 \pm 1.3 \pm 0.2_{\text{rad}}$	$21.4 \pm 1.3 \pm 0.6_{\text{SU}(2)}$
$2\pi^+2\pi^-$	$2m_\pi - 1.8$	$13.1 \pm 0.4 \pm 0.0_{\text{rad}}$	$12.3 \pm 1.0 \pm 0.4_{\text{SU}(2)}$
$\omega(782)$	$0.3 - 0.81$	$38.0 \pm 1.0 \pm 0.3_{\text{rad}}$	—
$\phi(1020)$	$1.0 - 1.055$	$35.7 \pm 0.8 \pm 0.2_{\text{rad}}$	—
Other excl.	$2m_\pi - 1.8$	$24.3 \pm 1.3 \pm 0.2_{\text{rad}}$	—
$J/\psi, \psi(2S)$	$3.08 - 3.11$	$7.4 \pm 0.4 \pm 0.0_{\text{rad}}$	—
$R$ [QCD]	$1.8 - 3.7$	$33.9 \pm 0.5_{\text{QCD}}$	—
$R$ [data]	$3.7 - 5.0$	$7.2 \pm 0.3 \pm 0.0_{\text{rad}}$	—
$R$ [QCD]	$5.0 - \infty$	$9.9 \pm 0.2_{\text{QCD}}$	—
sum	$2m_\pi - \infty$	$690.8(3.9)(1.9)_{\text{rad}}(0.7)_{\text{QCD}}$	$710.1(5.0)(0.7)_{\text{rad}}(2.8)_{\text{SU}(2)}$

The higher order (NLO) hadronic contributions  $a_\mu^{\text{had,NLO}}$  involve one hadronic vacuum polarization insertion with an additional loop (either photonic or leptonic or another hadronic vacuum polarization). They can be evaluated<sup>35</sup> with the same  $e^+e^- \rightarrow$  hadrons data sets used for  $a_\mu^{\text{had,LO}}$ . The numerical value<sup>36</sup> reads

$$a_\mu^{\text{had,NLO}} = -9.79(0.09)_{\text{exp}}(0.03)_{\text{rad}} \times 10^{-10} \quad (11)$$

where the first and second errors correspond respectively to the experimental uncertainty of the  $e^+e^-$  data and the radiative correction uncertainty.

Another higher order hadronic contribution to  $a_\mu$  is from the hadronic light-by-light scattering (illustrated with the lower figure in the second column in Fig. 1). Since it invokes a four-point correlation function, a dispersion relation approach using data is not possible at present. Instead, calculations<sup>37</sup> involving pole insertions (or Goldstone boson exchanges), short distance quark loops and charged pion (and kaon) loops have been individually performed in a large  $N_c$  QCD approach. A representative value used in Ref.<sup>20</sup> was  $a_\mu^{\text{had,LBL}} = 8.6(3.5) \times 10^{-10}$ .

A new analysis<sup>38</sup>, which takes into account the proper matching of asymptotic short-distance behavior of pseudoscalar and axial-vector contributions with the free quark loop behavior, leads to  $a_\mu^{\text{had,LBL}} = 13.6(2.5) \times 10^{-10}$ . However, as pointed out in Ref.<sup>39</sup>, several small but negative contributions such as charged pion loops and scalar resonances were not included in the latter calculation, thus in a recent update evaluation<sup>40</sup> of  $a_\mu$ , the following value

$$a_\mu^{\text{had,LBL}} = 12.0(3.5) \times 10^{-10} \quad (12)$$

was used<sup>c</sup>. This is consistent with the value  $a_\mu^{\text{had,LBL}} = 11(4) \times 10^{-11}$ , suggested in Ref.<sup>41</sup>. The uncertainty  $a_\mu^{\text{had,LBL}}$ , being the second largest one next to  $a_\mu^{\text{had,LO}}$ , clearly needs improvement in the near future.

Adding all SM contributions together, the comparison from recent evaluations<sup>21,36,42,43,44,40</sup> with the measurement is shown in Fig. 4. While the  $\tau$  data-based calculation agrees with the measurement within the errors, the  $e^+e^-$  data-based evaluations show a deviation of around 3.3 standard deviations.

<sup>c</sup>A different evaluation<sup>44</sup> used directly the value of Ref.<sup>38</sup> of  $13.6(2.5) \times 10^{-10}$ .

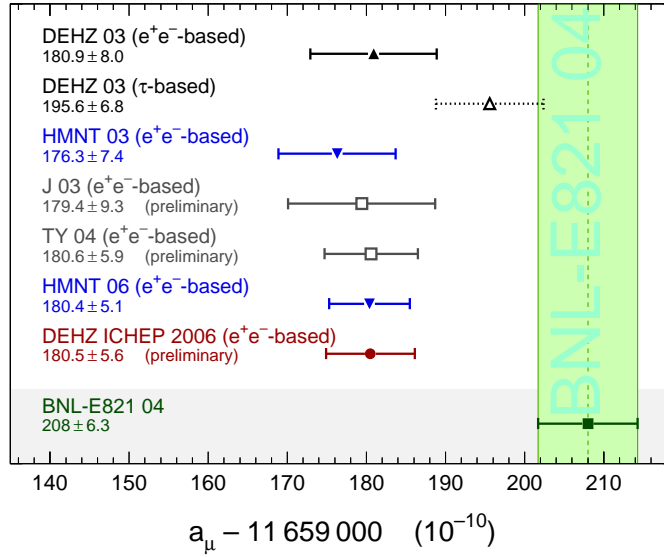


Figure 4: Comparison of recent theoretical evaluations of  $a_\mu$  with the BNL measurement.

## 4 Discussions

### 4.1 Tau Data versus $e^+e^-$ Data

The  $\tau$  data used in the  $a_\mu$  evaluation is the averaged one from the LEP experiments ALEPH<sup>45</sup> and OPAL<sup>46</sup> and the CLEO experiment<sup>47</sup>. The data are compared in Ref.<sup>19</sup> and found in good agreement in particular for the two most precise data from ALEPH and CLEO. These data are complementary as the ALEPH data are more precise below the  $\rho$  peak while CLEO has the better precision above.

A comparison between the averaged  $\tau$  data and the  $e^+e^-$  for the dominant  $\pi\pi$  mode is shown in Fig. 5. The difference of 5 – 10% in the energy region of  $0.65 - 1.0 \text{ GeV}^2$  is clearly visible. The difference with KLOE is even more pronounced.

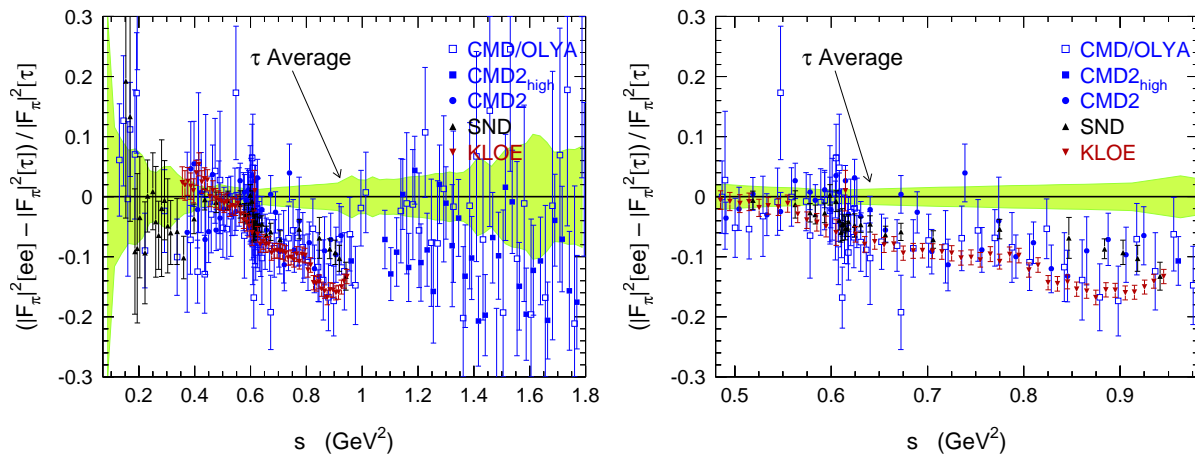


Figure 5: Relative comparison of the  $\pi^+\pi^-$  spectral functions from  $e^+e^-$ -annihilation data and isospin-breaking-corrected  $\tau$  data, expressed as a ratio to the  $\tau$  spectral function. The shaded band indicates the errors of the  $\tau$  data. The right hand plot emphasizes the region of the  $\rho$  peak.

## 4.2 CVC

An alternative way of comparing  $\tau$  and  $e^+e^-$  data is to compare measurements of branching fractions  $B$  in  $\tau$  decays with their expectations from CVC (Conserved Vector Current) using  $e^+e^-$  spectral functions, duly corrected for isospin breaking effects. The advantage of a such comparison is that the measurements of  $B$  are more robust than the spectral functions as the latter ones depend on the experimental resolution and require a numerically delicate unfolding.

The comparison for  $\pi\pi$  mode revealing a discrepancy of 4.5 standard deviations is shown in Fig. 6. Similar comparisons for decay modes  $\tau^- \rightarrow \nu_\tau \pi^- 3\pi^0$  and  $\tau^- \rightarrow \nu_\tau 2\pi^- \pi^+ \pi^0$  have also been made and the differences with the corresponding  $e^+e^-$  data are found respectively at 0.7 and 3.6 standard deviations.

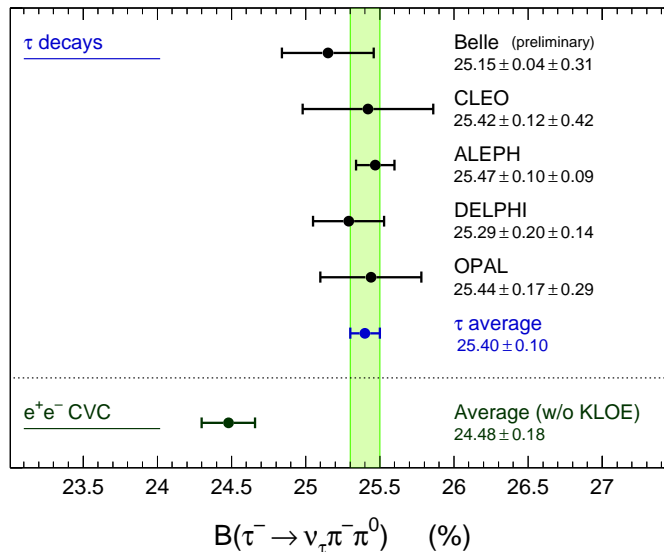


Figure 6: The measured branching fractions for  $\tau^- \rightarrow \nu_\tau \pi^- \pi^0$  compared to the expectation from the  $e^+e^- \rightarrow \pi^+ \pi^-$  spectral function applying the isospin-breaking correction factors.

## 5 Conclusion and Prospects

The muon magnetic anomaly  $a_\mu$  is one of the most precisely known quantities both experimentally and theoretically in the SM. Incorporating new  $e^+e^-$  data from CMD2 and SND for  $\pi\pi$  mode and from BABAR for multihadronic modes, new SM determinations of  $a_\mu$  have been obtained with a theoretical precision exceeding for the first time in recent years the experimental one. The SM prediction is found to be smaller than the measurement by about 3.3 standard deviations. Unfortunately one can not draw a definitive conclusion for the moment as the  $\tau$  data based prediction is in agreement with the measurement.

Therefore it is extremely important that one clarifies the discrepancy between the  $e^+e^-$  and  $\tau$  data in particular on the  $\pi\pi$  mode. There are a number of possibilities: (1) (the normalization of) the  $e^+e^-$  data is wrong, (2) the tau data are wrong, (3) both are correct but there are unaccounted effects<sup>48</sup> which explain the discrepancy between the two.

Possibility (1) may be also related to the current difference (mainly on the shape of the spectral functions) between CMD2/SND data and KLOE data obtained respectively from the beam energy scan method and the radiative return method. This difference is expected to be resolved soon as KLOE has more and high quality data to be analyzed. In addition, reduced systematics uncertainties can be achieved if the measurement is made by normalizing the  $\pi\pi$

data to  $\mu\mu$  instead of to luminosity using the large angle Bhabha process.

The long awaited high precision measurement in  $\pi\pi$  mode from BABAR using also the radiative return method will certainly help in clarifying some of the issues.

On the tau side, further improvement on the high mass part of the spectral functions is expected from large statistical data samples available at  $B$  factories and a  $\tau$ -charm factory.

While the leading hadronic uncertainty gets improved with the forthcoming high precision  $e^+e^-$  (and  $\tau$ ) data, the next item awaiting for significant improvement concerns the uncertainty on the light-by-light scattering contribution  $a_\mu^{\text{had,LBL}}$ .

Given the fact that the theoretical error is already smaller than the experimental one, it is timely to improve the latter. Indeed there is a new project BNL-E969 allowing to reduce the current error by more than a factor two down to 0.24 ppm. We are looking forward that the project gets funded very soon.

## Acknowledgments

The author wishes to thank the organizers of the conference for the invitation and M. Davier, S. Eidelman and A. Höcker for the fruitful collaboration.

## References

1. J.P. Miller, E. de Rafael and B. Lee Roberts, *RPP* **70**, 795 (2007).
2. R.L. Garwin, L.M. Lederman and M. Weinrich, *Phys. Rev.* **105**, 1415 (1957).
3. R.L. Garwin, D.P. Hutchinson, S. Penman and G. Shapiro, *Phys. Rev.* **118**, 271 (1960).
4. G. Charpak *et al.*, *Phys. Rev. Lett.* **6**, 128 (1961), *Nuovo Cimento* **22**, 1043 (1961), *Phys. Lett.* **1**, 16 (1962), *Nuovo Cimento* **37**, 1241 (1965).
5. G. Charpak *et al.*, *Phys. Lett.* **1**, 16 (1962).
6. J. Bailey *et al.*, *Phys. Lett. B* **28**, 287 (1968).
7. J. Bailey *et al.*, *Phys. Lett. B* **55**, 420 (1975).
8. J. Bailey *et al.*, *Nucl. Phys. B* **150**, 1 (1979).
9. H.N. Brown *et al.* (Muon ( $g-2$ ) Collaboration), *Phys. Rev. D* **62**, 091101 (2000).
10. H.N. Brown *et al.* (Muon ( $g-2$ ) Collaboration), *Phys. Rev. Lett.* **86**, 2227 (2001).
11. G.W. Bennett *et al.* (Muon ( $g-2$ ) Collaboration), *Phys. Rev. Lett.* **89**, 101804 (2002).
12. G.W. Bennett *et al.* (Muon ( $g-2$ ) Collaboration), *Phys. Rev. Lett.* **92**, 161802 (2004).
13. G.W. Bennett *et al.* (Muon ( $g-2$ ) Collaboration), *Phys. Rev. D* **73**, 072003 (2006).
14. G. Gabrielse *et al.*, *Phys. Rev. Lett.* **97**, 030802 (2006).
15. T. Kinoshita and M. Nio, *Phys. Rev. D* **73**, 053007 (2006).
16. J. Schwinger, *Phys. Rev.* **73**, 416 (2004).
17. M. Gourdin and E. de Rafael, *Nucl. Phys. B* **10**, 667 (1969).
18. S.J. Brodsky and E. de Rafael, *Phys. Rev.* **168**, 1620 (1968).
19. M. Davier, A. Höcker and Z. Zhang, *Rev. Mod. Phys.* **78**, 1043 (2006).
20. M. Davier, S. Eidelman, A. Höcker and Z. Zhang, *Eur. Phys. J. C* **27**, 497 (2003).
21. M. Davier, S. Eidelman, A. Höcker and Z. Zhang, *Eur. Phys. J. C* **31**, 503 (2003).
22. A. Quenzer *et al.* (DM1 Collaboration), *Phys. Lett. B* **76**, 512 (1978).
23. I.B. Vasserman *et al.* (TOF Collaboration), *Sov. J. Nucl. Phys.* **33**, 368 (1981).
24. I.B. Vasserman *et al.* (OLYA Collaboration), *Sov. J. Nucl. Phys.* **30**, 519 (1979).
25. L.M. Barkov *et al.* (OLYA and CMD Collaborations), *Nucl. Phys. B* **256**, 365 (1985).
26. D. Bisello *et al.* (DM2 Collaboration), *Phys. Lett. B* **220**, 321 (1989).
27. R.R. Akhmetshin *et al.* (CMD2 Collaboration), *Phys. Lett. B* **578**, 285 (2004).
28. A. Aloisio *et al.* (KLOE Collaboration), *Phys. Lett. B* **606**, 12 (2005).

29. M.N. Achasov *et al.* SND Collaboration, *J. Exp. Theor. Phys.* **103**, 380 (2006) [hep-ex/0605013].
30. R.R. Akhmetshin *et al.* (CMD2 Collaboration), *J. Exp. Theor. Phys. Lett.* **84**, 413 (2006) [hep-ex/0610016].
31. R.R. Akhmetshin *et al.* (CMD2 Collaboration), [hep-ex/0610021].
32. V.M. Aulchenko *et al.* (CMD2 Collaboration), *J. Exp. Theor. Phys. Lett.* **82**, 743 (2005) [hep-ex/0603021].
33. B. Aubert *et al.* (BABAR Collaboration), *Phys. Rev. D* **70**, 072004 (2004), *Phys. Rev. D* **71**, 052001 (2005), *Phys. Rev. D* **73**, 052003 (2006).
34. R. Alemany, M. Davier and A. Höcker, *Eur. Phys. J. C* **2**, 123 (1998).
35. B. Krause, *Phys. Lett. B* **390**, 392 (1997).
36. K. Hagiwara, A.D. Martin, D. Nomura and T. Teubner, *Phys. Rev. D* **69**, 093003 (2004).
37. J. Bijnens, E. Pallante and J. Prades, *Nucl. Phys. B* **474**, 379 (1996), *Nucl. Phys. B* **626**, 410 (2002), M. Hayakawa, T. Kinoshita and A.I. Sanda, *Phys. Rev. D* **54**, 3137 (1996), M. Hayakawa and T. Kinoshita, *Phys. Rev. D* **57**, 465 (1998), *Phys. Rev. D* **66**, 019902(E) (2002), I. Blokland, A. Czarnecki and K. Melnikov, *Phys. Rev. Lett.* **88**, 071803 (2002), M. Knecht and A. Nyffeler, *Phys. Rev. D* **65**, 073034 (2002), M. Knecht *et al.*, *Phys. Rev. Lett.* **88**, 071802 (2002).
38. K. Melnikov and A. Vainshtein, *Phys. Rev. D* **70**, 113006 (2004).
39. M. Davier and W.J. Marciano, *Annu. Rev. Nucl. Part. Sci.* **54**, 115 (2004).
40. M. Davier, to appear in *Proceedings of 9th International Workshop on Tau Lepton Physics (Tau06)*, Pisa, Italy, 19-22 Sep 2006.
41. J. Bijnens and J. Prades, hep-ph/0702170.
42. F. Jegerlehner, *Nucl. Phys. B (Proc. Suppl.)* **131**, 213 (2004)
43. J.F. de Trconiz and F.J. Yndurain, *Phys. Rev. D* **71**, 073008 (2005).
44. K. Hagiwara, A.D. Martin, D. Nomura and T. Teubner, hep-ph/0611102.
45. S. Schael *et al.* (ALEPH Collaboration), *Phys. Rept.* **421**, 191 (2005).
46. K. Ackerstaff *et al.* (OPAL Collaboration), *Eur. Phys. J. C* **8**, 183 (1999).
47. S. Anderson *et al.* (CLEO Collaboration), *Phys. Rev. D* **61**, 112002 (2000), K.W. Edwards *et al.* (CLEO Collaboration), *Phys. Rev. D* **61**, 072003 (2000).
48. M.V. Chizhov, hep-ph/0311360.

